On the Theoretical Performance Limits of Long Repeated/Regenerated Optical IMDD Links

Fredy Francis (ee14d020@ee.iitm.ac.in)
IIT Madras: Indian Institute of Technology Madras https://orcid.org/0000-0003-3083-7445
Manivasakan R
IIT Madras: Indian Institute of Technology Madras

Research Article

Keywords: Optical Amplifiers, EDFA, Optical Regenerators, BER, SNR, Performance analysis

Posted Date: July 22nd, 2021

DOI: https://doi.org/10.21203/rs.3.rs-615471/v1

Noname manuscript No.
(will be inserted by the editor)

On the Theoretical Performance Limits of Long Repeated/Regenerated Optical IMDD Links

Fredy Francis · **R Manivasakan**

Received: date / Accepted: date

Abstract The introduction of optical amplifiers has drastically increased the capacity and the reach of optical transmission links. However, they add Amplified Spontaneous Emission (ASE) noise, which progressively degrades the Signal to Noise Ratio (SNR) when cascaded and ultimately limits the transmission reach and performance. This is conventionally offset using regenerators, typically Optical-Electrical-Optical (OEO) conversion devices, that recreate the signal restoring its source SNR, albeit with bit errors due to the hitherto accumulated noise. These OEO regenerators tend to be expensive and add to the link latency, which sets the scene for widespread commercial implementation of all-optical regenerators in the near future. Our work aims to analyze the ideal, best-case theoretical gains achievable using an all-regenerator optical link as compared to an all-repeater link. So, this analytical study serves as a benchmark against which future link performance gains can be compared. We also translate this bound on BER advantage to extra reach or lower transmission power. We compare and contrast the evolution of noise power and BER down the link using the derived analytical expressions. The theoretical comparative study is then evaluated by incorporating the physical parameters of the devices. Both results agree and prove the dramatic increase in link reach achievable using all-regenerator links with minor input power penalties. Further, certain approximations to reduce the computational overhead for the described methods are proposed, which should find applications in dynamic reconfigurable optical networks.

Keywords Optical Amplifiers · EDFA · Optical Regenerators · BER · SNR · Performance analysis

1 Introduction

Optical networks are now ubiquitous and of cardinal significance in today's high-speed communication infrastructure, owing to their huge bandwidth, low losses, excellent Electromag-

Fredy Francis
Indian Institute of Technology Madras, Department of Electrical Engineering, Chennai, India, 600036
E-mail: ee14d020@ee.iitm.ac.in

R Manivasakan
Indian Institute of Technology Madras, Department of Electrical Engineering, Chennai, India, 600036

netic Interference (EMI) performance, small size, and flexibility [2], [4]. Fiber optics are deployed not just in the backbone network but also in applications such as optical fronthauling for 5G wireless data transport [28], [18], [7]. The introduction of the EDFA in the early 1990s was a major advancement as the amplification could be achieved in the optical domain and hence avoiding the cumbersome and costly OEO conversion [10], [26]. Further, EDFA has a broad bandwidth and hence could amplify different wavelength channels simultaneously, which paved the way for WDM in Intensity Modulated Direct Detection (IMDD) systems and resulted in an explosion of available fiber bandwidth capacity [11].

EDFA (interchangeably referred to as optical repeater, 1R regenerator in this work) works on the principle of stimulated emission, and hence the inevitable spontaneous emissions add to the signal as noise [9] [2]. This degrades the SNR, and in the case of long cascaded links, the noise keeps accumulating, which fundamentally limits the optical link reach [29]. Further, these long repeated links also aggravate other impairments like nonlinearities and dispersion. For example, Self Phase Modulation (SPM) may put an upper bound on the allowed transmitting power (and repeater gain) for a reasonably long (say $>$10 repeater) link [2]. Hence OEO Regenerators had to be introduced after several repeaters to rebuild the signal, restoring its SNR. These early OEO optoelectronic regenerators can be thought of as receive-transmit pairs, which would detect the signal, makes the bit decisions, and then transmits the bits towards the receiver of the optical link [27]. This would add bit errors, owing to the noisy input, but increase the optical reach significantly. Subsequently, the BER accumulation may prove to be the limiting factor. Regenerator spacing was typically around 600-800 km at the dawn of the millennia [2], which have since increased.

However, other than introducing bit errors, these optoelectronic regenerators are bandwidth limiting, expensive and their implementation with WDM can be complex and challenging, as each channel has to be individually demultiplexed and processed separately [16]. This opens up huge opportunities for all Optical Regenerators: high speed, low latency, lower-powered replacements, which can also handle different modulation formats [20], [12]. But these all-optical 3R regenerator technologies are yet to mature, though lots of commendable works are being reported [17], [23], [24], [25].

This paper proposes some abstract models for EDFA, OEO Regenerators, and all-optical regenerators to compare and contrast their absolute performance advantages. We derive and compare the theoretical BER performance limits for all-regenerator/repeater links and interpret those results around physical considerations. Then we reinterpret the BER advantage of all-regenerator link in-terms of extra reach and lower signal powers. These raw performance estimates can be used to benchmark advancements in the current hybrid repeater regenerator systems and future all-optical regenerator systems. They can also serve as a baseline for more involved analysis, including advanced modulation schemes. Next, we have considered some typical EDFA physical parameters and various noise mechanisms at the detector to derive the expressions for a more realistic link. Further, some approximations are explored that can improve the computational performance of the above analysis. We conclude by providing more insights into the results that we obtained.

One of the earliest studies of noise accumulation comparison is done by Schiess et.al. [27], where pulse shape evolution and noise evolution were compared between analog OEO repeaters and EDFA links. Ohlen et al. [22] proved that even a small nonlinearity in an optoelectronic repeater response could reduce BER accumulation compared to their linear counterparts. These works [27], [22] predated optical regenerators and were meant to compare EDFA links and OEO repeaters (not regenerators - which generally included clock recovery and decision logics) with added nonlinearities for noise suppression. Mork et al. [21] derived approximate analytical expressions for BER in cascaded all-optical 2R regenerators

and shows even moderate reshaping can significantly reduce noise build-up. Zhu et al. [30] extend this by investigating timing jitter and pattern dependence. Later, cascaded operation of 50 MZI-SOA based 3R regenerator over an advanced modulation is detailed in Ref [15]. Cascaded burst mode optical 2R regenerators are modeled in Ref [8]. However, in all the above works, the model used is complicated, implementation-specific, and the bit-inversion along the link is not considered. We propose a more general, simplistic, lightweight model considering the bit-inversion down the link. The proposed model should apply to any ideal IMDD (current and future) 3R regenerator irrespective of the underlying implementation technology.

The paper is organized as follows: Section 2 introduces the theoretical analysis based on some assumptions. Section 3, introduces some Q function approximations and its application to the problem. Section 4 deals with more physical aspects of the problem and introduces various noise mechanisms and BER analysis. Sections 5 and 6 describes various results and inferences from sections 2 and 4 respectively.

2 Theory - Ideal BER Performance

We first derive the abstract BER performance of all-repeater and all-regenerator links without looking into its causes [19], which is later explored in section 4. Note that we use EDFA/Repeater/Amplifier interchangeably and not to be confused with some literature terming regenerator (here) as a repeater.

2.1 All (1R) Repeater Link

Consider an 'M' repeated distortionless all-repeated link, with each repeater providing just enough gain to offset the losses of the preceding section. As the SNR degrades gradually, we have,

$$SNR_m = \frac{SNR_1}{M} \tag{1}$$

where $SNR_1 (\triangleq \left(\frac{S}{N}\right)_1)$ is the SNR after single hop for simple modulation schemes (ON-OFF signalling or BPSK or Binary PAM) as given by [5]. Correspondingly we have the probability of error (BER) as,

$$P_e^{rep} = Q\left[\sqrt{\frac{1}{M}\left(\frac{S}{N}\right)_1}\right] \tag{2}$$

These relations show the progressive noise build-up and its implications on BER as the link extends further. So, the input power has to be linearly increased with link length to maintain the target BER, which can introduce Kerr-non-linearity and deteriorate the performance.

2.2 All 3R Regenerator Link

It is rather the bit errors that add up one hop to the next in an all-regenerated link. Define BER after a single hop to be [2],

$$BER_1 = \alpha = Q\left[\sqrt{\left(\frac{S}{N}\right)_1}\right] \tag{3}$$

Now, analysing using results from sec 11.2 of [5] the BER of M regenerator link, P_e^{reg}, can be expressed as,

$$P_e^{reg} = \sum_{i\,\text{odd}\&<=M} P_l(i) = \binom{M}{1}\alpha(1-\alpha)^{M-1} + \binom{M}{3}\alpha^3(1-\alpha)^{M-3} + \ldots + \binom{M}{l}\alpha^l(1-\alpha)^{M-l} \quad (4)$$

where, l is the largest odd number $<= M$. When $\alpha << 1$ and M is not too larger, which are very reasonable approximations in our case, this can be approximated to,

$$P_e^{reg} \approx M\alpha \quad (5)$$

So, it is evident that in all 3R regenerator cases, BER build-up is much more gradual and manageable compared to the SNR degradation-based BER of all-repeater links. This is further evident in the results section 5.

2.3 Improvement in Transmission Reach

The BER superiority of the all-regenerator link can be made to translate into other gains, like increased link reach or reduced transmit powers. Towards computing the extra reach afforded by the all-regenerator link, we equate the RHS of Eq. 2 and Eq. 4 and numerical solve for the number of stages (M_{rep} and M_{reg}) for both cases at different values of SNR, as given below.

$$Q\left[\sqrt{\frac{1}{M_{rep}}\left(\frac{S}{N}\right)}\right] = \binom{M_{reg}}{1}\alpha(1-\alpha)^{M_{reg}-1} + \binom{M_{reg}}{3}\alpha^3(1-\alpha)^{M_{reg}-3} + \ldots + \binom{M_{reg}}{l}\alpha^l(1-\alpha)^{M_{reg}-l} \quad (6)$$

where l is the largest odd term $<= M_{reg}$, and α is the single hop BER. The results are detailed in section 5.

2.4 Reduction in Launched Power

Again, we try to translate the BER advantage of the all-regenerator link to reduce the transmitted power, which may even help reduce nonlinearities of the link if it had a high transmit power to start with. We calculate and visualize this by computing the SNR levels that could equate both schemes' BER performance and plot their ratio at different link lengths. So we have,

$$Q\left[\sqrt{\frac{1}{M}(SNR_{rep})_1}\right] = \sum_{odd\,i}^{l}\binom{M}{i}\alpha^i(1-\alpha)^{M-i} \quad (7)$$

where $\alpha = Q\left[\sqrt{SNR_{reg}}\right]$ and l is the largest odd term $<= M$. Given M and SNR_{rep}, numerically SNR_{reg} is searched to satisfy the equality and is repeated for various M. As can be seen in the results section, significant power savings can be had. Note, this does not take into consideration the wall plug efficiency of the repeater/regenerator devices.

3 Approximate Expressions for BER

The physical interpretation (that regenerator's case is better, which is intuitive) is not immediately evident from expressions derived in the last section, mainly because the Q function, being an integral, is computationally intensive to compute. This section uses approximations to the Q function available in the literature to solve the above problems. The approximate expression for BER is derived using the Q function approximations. The results of this section could be used in simulation / computational software modeling these systems.

We begin from the approximate expression in Eq. 5 and conjuncture it to be true for high enough values of SNR, ie,

$$MQ\left(\sqrt{SNR}\right) < Q\left(\sqrt{\frac{SNR}{M}}\right) \tag{8}$$

We use different Q function approximations on this and see how well it performs in the results section.

3.1 Derivation for BER using Approximations for Q() function by Chiani et al.

Chiani et al. have proposed that [6],

$$Q(x) \approx \frac{1}{12}e^{-\frac{x^2}{2}} + \frac{1}{4}e^{-\frac{2x^2}{3}} \quad \forall x > 0$$

Using this on Eq. 8 with x taking $\frac{\sqrt{S}}{\sqrt{2\sigma_N^2}}$ for regenerators and $\frac{\sqrt{S}}{\sqrt{2M\sigma_N^2}}$ for repeaters. So we have,

$$M\left(\frac{1}{12}e^{-\frac{\left(\frac{S}{2\sigma_N^2}\right)}{2}} + \frac{1}{4}e^{-\frac{2\left(\frac{S}{2\sigma_N^2}\right)}{3}}\right) < \left(\frac{1}{12}e^{-\frac{\left(\frac{S}{2M\sigma_N^2}\right)}{2}} + \frac{1}{4}e^{-\frac{2\left(\frac{S}{2M\sigma_N^2}\right)}{3}}\right) \tag{9}$$

3.2 Derivation for BER using Approximations for Q() function by Karagiannidis et al.

A tighter bound of Q can be found in the works of Karagiannidis et al., given by [14],

$$Q(x) \approx \frac{\left(1-e^{-1.4x}\right)e^{-\frac{x^2}{2}}}{1.135\sqrt{2\pi}x} \quad \forall x \geq 0$$

Following similar steps from last time, we get,

$$M\left(\frac{\left(1-e^{-1.4\left(\sqrt{\frac{S}{2\sigma_N^2}}\right)}\right)e^{-\frac{\left(\frac{S}{2\sigma_N^2}\right)}{2}}}{1.135\sqrt{2\pi}\left(\sqrt{\frac{S}{2\sigma_N^2}}\right)}\right) < \left(\frac{\left(1-e^{-1.4\left(\sqrt{\frac{S}{2M\sigma_N^2}}\right)}\right)e^{-\frac{\left(\frac{S}{2M\sigma_N^2}\right)}{2}}}{1.135\sqrt{2\pi}\left(\sqrt{\frac{S}{2M\sigma_N^2}}\right)}\right) \quad \text{for} M, \frac{S}{\sigma_N^2} > 0 \tag{10}$$

Which when simplified and rearranged gives,

$$\sqrt{M}\left(1-e^{-1.4\sqrt{\frac{S}{2\sigma_N^2}}}\right)e^{-\frac{S}{4\sigma_N^2}} < \left(1-e^{-1.4\sqrt{\frac{S}{2M\sigma_N^2}}}\right)e^{-\frac{S}{4M\sigma_N^2}} \tag{11}$$

3.3 Derivation for BER using Approximations for Q() function by Abreu et al.

Tight bounds from Abreu et al. have upper and lower bounds, and the 'tightness' can be adjusted using different parameters. From [1] we have,

$$\frac{e^{-x^2}}{a_L}+\frac{e^{-\frac{x^2}{2}}}{b_L(x+1)} \leq Q(x) \leq \frac{e^{-x^2}}{a_U}+\frac{e^{-\frac{x^2}{2}}}{b_U(x+1)} \tag{12}$$

We have used the following parameters [1], $b_L \geq \sqrt{2\pi} = 2.5$ and $a_L = \frac{8b_L\sqrt{2\pi}exp(-0.5)}{4b_L-3\sqrt{2\pi}} \approx 12.16$, $a_U = 48.9$ and $b_U = 2$, and we have,

$$\frac{e^{-x^2}}{12.16}+\frac{e^{-\frac{x^2}{2}}}{2.5(x+1)} \leq Q(x) \leq \frac{e^{-x^2}}{48.9}+\frac{e^{-\frac{x^2}{2}}}{2(x+1)} \tag{13}$$

As this has both upper and lower limits, we have chosen the worst case for comparison: using the lower bound for repeater and the upper bound for regenerators. Making the substitutions based on this, we have,

$$M\left(\frac{e^{-\frac{S}{2\sigma_N^2}}}{48.9}+\frac{e^{-\frac{S}{4\sigma_N^2}}}{2\left(\sqrt{\frac{S}{2\sigma_N^2}}+1\right)}\right) < \frac{e^{-\frac{S}{2M\sigma_N^2}}}{12.16}+\frac{e^{-\frac{S}{4M\sigma_N^2}}}{2.5\left(\sqrt{\frac{S}{2M\sigma_N^2}}+1\right)} \tag{14}$$

Resulting plots and further comments are provided in sec 5.2.

4 Analytical Performance of Realistic Long Repeated Optical IMDD Link

In this section, we look into more physical and practical aspects of the optical link design. Noise mechanisms within the amplifier and detector are briefly introduced, and the abstract results introduced in the previous section are given a more physical dimension. Note that in this section, we have modeled a regenerator as a transmit-receiver pair; hence its analysis is more in line with optoelectronic regenerators.

4.1 BER at Receiver

The photodetector's primary noise mechanisms involve the shot noise arising from the randomness of photon reception, thermal noise due to electrons, and the dark current of the photodiode. The SNR at the detector is defined as [2],

$$SNR = \frac{\text{average signal power}}{\text{noise power}} = \frac{I_p^2}{\sigma^2} \tag{15}$$

where P_{in} is incident optical power, $I_p = R_d P_{in}$ is the photocurrent with R_d the responsivity. σ^2 is the net noise power comprised of thermal ($\sigma_T^2 = 4(k_B T/R_L)F_n \Delta f$) and shot noise ($\sigma_s^2 = 2q(R_d P_{in} + I_d)$) while neglecting the dark current. Other constants have their usual meanings, k_B - Boltzmann constant, q the charge of electron, T - temperature, R_L - load resistance, F_n - amplifier noise figure at receiver, and Δf - effective noise bandwidth.

The BER of an Intensity-Modulation, Direct Detection (IMDD) system with '0' and '1' is transmitted with uniform probability, and Gaussian distributed thermal and short noise is given by [2],

$$BER = P_e = \frac{1}{2} erfc\left(\frac{Q}{\sqrt{2}}\right) \tag{16}$$

where, $Q = \frac{I_1 - I_0}{\sigma_1 + \sigma_0}$. I_0 and I_1 are the signal intensities representing '0' and '1' levels. σ_0 and σ_1 represent the corresponding values for net noise variance. In case of thermal noise limited system (which is mostly the case), we have $\sigma_0 = \sigma_1 = \sigma$, and making the reasonable assumptions of $I_0 = 0$ we have,

$$Q = \frac{I_1}{2\sigma} = \frac{\sqrt{SNR}}{2} \tag{17}$$

Which along with Eq. 16 gives,

$$BER = \frac{1}{2} erfc\left(\frac{\sqrt{SNR}}{2\sqrt{2}}\right) \tag{18}$$

4.2 Regenerator noise analysis

As discussed before, although the regenerator restores the SNR, it adds bit errors into the stream. Following the analysis of section 2.2 but using parameters from section 4.1, we have for a single-stage,

$$BER_1 = \beta \triangleq \frac{1}{2} erfc\left(\frac{\sqrt{SNR_{reg}}}{2\sqrt{2}}\right) \tag{19}$$

Modelling the optoelectronic regenerator as a receive-transmit pair, we have the detector noise at the receiver. So [2],

$$SNR_{reg} = \frac{(RP_{in})^2}{\sigma_T^2 + \sigma_s^2} \tag{20}$$

Now we use this in the analysis of section 2.2, with l being the largest odd number $<= M$. Using Eq. 19 and Eq. 4 we get,

$$BER_{reg}^M = \sum_{i\,\text{odd}\,\&<M} P_l(i) = \binom{M}{1}\beta(1-\beta)^{M-1} + \binom{M}{3}\beta^3(1-\beta)^{M-3} + \ldots + \binom{M}{l}\beta^l(1-\beta)^{M-l} \tag{21}$$

which, as before, becomes $M\beta$ for $\beta << 1$ and M not too large. So we have,

$$BER_{reg}^M \approx \frac{M}{2} erfc\left(\frac{\sqrt{SNR_{reg}}}{2\sqrt{2}}\right) \tag{22}$$

4.3 Repeater noise analysis

Here we look into the noise mechanism of an EDFA (the most popular repeater in optical links) and how it manifests into bit errors at the detector. The spontaneously emitted photons from the EDFA, which end up in the same direction and mode of the signal, get amplified and travel down the link, accumulating over until it is detected. At the detector, these photons beat with the signal, causing noise in the photocurrent generated. If E_{in} and E_{sp} represent the signal field and spontaneous emission field respectively, we have the net photocurrent generated at the detector as [2],

$$I = R|\sqrt{G}E_{in} + E_{sp}|^2 \tag{23}$$

where G is the amplifier gain. As both fields oscillate at different frequencies and random phase, the beat noise current can be given by [2],

$$\Delta I = 2R\sqrt{GP_{in}}|E_{sp}|\cos\theta \tag{24}$$

where, θ is random and varies rapidly. So, after averaging over, we get the noise variance due to ASE as [2],

$$\sigma^2_{ASE} \approx 4(RGP_{in})(RS_{sp})\Delta f \tag{25}$$

$S_{sp}(\nu)$ is the spontaneous emission noise spectrum, which is typically white and is given by [2],

$$S_{sp}(\nu) = (G-1)n_{sp}h\nu \tag{26}$$

where n_{sp} is the population inversion factor (or spontaneous emission factor), h is the Planck's constant, ν is the optical frequency. Also, $n_{sp} = \frac{N_2}{N_2 - N_1}$ where N_1 and N_2 corresponds to atomic densities at ground and excited states respectively.

So finally, considering the other noise sources along with ASE as well, we have at the detector of an all-repeater link,

$$SNR^M_{rep} = \frac{<I>^2}{\sigma^2} = \frac{(RP_{in})^2}{\sigma^2_T + \sigma^2_s + M\sigma^2_{ASE}} \tag{27}$$

And correspondingly,

$$BER^M_{rep} = \frac{1}{2}erfc\left(\frac{\sqrt{SNR^M_{rep}}}{2\sqrt{2}}\right) \tag{28}$$

is the expression for effective BER for M all-repeater optical link.

5 Performance of Ideal Long Repeated Optical Link - Numerical Results

In this section, we consider the ideal all-repeater and all-regenerator links (without getting into the more practical optical link to the level of parameters of its components), compute and present the performance corresponding to analytical expressions derived in sections 2 and 3 (Results corresponding to both exact expressions and approximations are given). Approximations are intended to reduce computational complexity scarifying some level of accuracy.

5.1 Exact Expressions for Performance of Ideal Long Repeated Optical Links

In this subsection, we use the (exact) expressions for performance described in Sec. 2. We begin by plotting BER accumulation for all-repeater and all-regenerator link against SNR (at M=10) (Eq. 2 and Eq. 4 respectively) and is shown in Fig. 1a. As expected, the performance of both links improved with larger SNR, but the all-regenerator link significantly outperforms its counterpart. This demonstrates that the periodic addition of few bit errors along the link is preferable over the gradual SNR degradation caused by the ASE accumulation, which ultimately gets converted into significantly higher BER at the receiver. Note that SNR is plotted in linear scale for consistency; using log scale would give the typical waterfall plot.

BER accumulation along the link for both cases are plotted next in Fig. 1b using the same equations but plotting it against the number of repeater/regenerator M (at SNR=30). This differs from the previous plot in that, for all-repeater links, the degraded SNR is converted to BER at each node and compared against the corresponding BER for the all-regenerator link. Again, it is profusely evident that the all-regenerated link outperforms the other, meaning it will be much more scalable and future-proof. The slope of the curves can be thought of as the BER accumulation rate along the link, which is, of course, much worse for the repeater link.

Figure.1c shows that BER accumulates much slowly in all-regenerator links and hence supports much longer links (larger number of M for the same target BER at the receiver). This is, of course, expected, as the all-repeater link was shown to have a much higher BER accumulation rate, which soon breaches the acceptable target BER. The SNR was limited to somewhere below 25 as the corresponding M for the all-regenerator link becomes large enough to cause memory issues during simulation. The approximations discussed above can help to get over the limitations. Here, we have used a conservative Forward Error Correction (FEC) limit of 10^{-5} as the target BER at the receiver of both links [3]. The results are based on the analysis given in section 2.3. Targetting a further lower BER, the performance contrast only widens.

We also compare the relative power requirements for both cases while targetting the same BER with the same number of repeater/regenerator (M) as described in section 2.4. For this, we plot the ratio of SNR requirement for both cases against link reach (Fig. 1d) and observes that this grows exponentially, signifying drastically lower power requirements for the latter.

5.2 Approximate Expressions for Performance of Ideal Long Repeated Optical Links

In this sub-section, approximate expressions for the performance measures are used, wherein the accuracy is traded off for the reduced computational overhead. Though this is not crucial for the design of static optical networks, for dynamic optical networks design [13], it might find an application. There are two instances in which the approximations are made: (a) when the binomial BER is approximated as in Eq. 5 (of course, it is only for all-regenerator case). (b) when the approximations for Q(x) are made. In this section, only (b) is addressed. On passing, we note that the all-repeater link's expressions are more accurate (approximation error is less) than the all-regenerator case.

We present the results and comparisons of approximations as described in section 3 for M = 10. In general, the approximations are a bit inaccurate for lower SNR values, but as it is unusual for an optical link to work under such low SNRs, this can be ignored. We

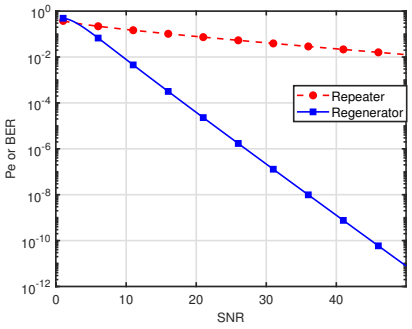

(a) BER vs SNR for all-Repeater/Regenerator links

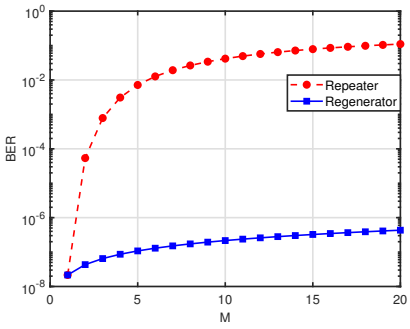

(b) BER accumulation for Repeater/Regenerator links (SNR = 30)

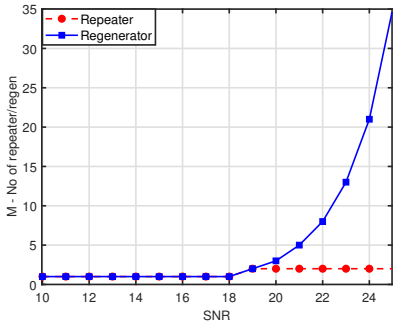

(c) Reach for Repeater/Regenerator links (target BER of 10^{-5})

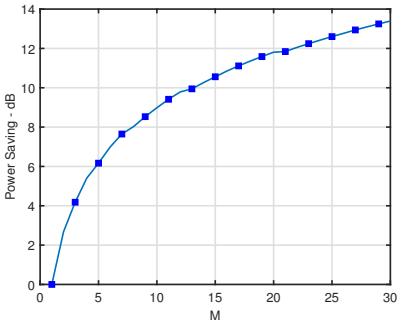

(d) Power savings when using M regenerators over M repeaters (BER target = 10^{-5})

Fig. 1: Ideal link performance evaluation for all Repeater/Regenerator cases

start by plotting the results using our conjuncture approximation (only approximated for the binomial expansion, not for Q function) in Eq. 8 to serve as the baseline (Fig. 2a). In Fig. 2b, we plot the BER vs. single-hop SNR for fixed M (=10), wherein we use the Chiani et al.'s approximation for Q() function. Similarly, in Fig. 2c, we use Karagiannidis et al approximation for Q() function.

Abreu et al.'s approximation is expected to be tighter, and with the parameter values chosen in Sec. 3.3 it gives good accurate results (Fig. 2d). It also has the additional benefit of adjusting the 'tightness' of the bounds and has upper and lower bound values. Note that here we have plotted the higher bound for regenerator BER vs. the lower bound for repeater BER, which would be the worst-case scenario for performance contrast.

6 Numerical Results Corresponding to Analytical Performance of Realistic Long Repeated Optical IMDD Link.

This section pertains to the case of the realistic optical link. The physical parameters of the associated optical components (modeling the repeater or regenerator and receiver) are explicitly considered as given in Sec 4. We use the following values for various parameters in

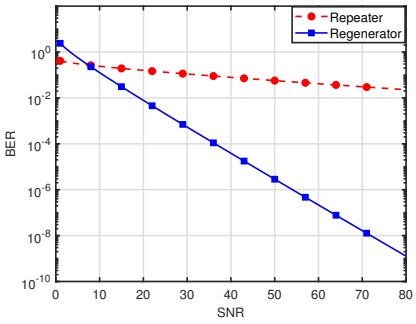

(a) Numerical Verification of Conjecture Eq. 8 - BER vs SNR for M = 10

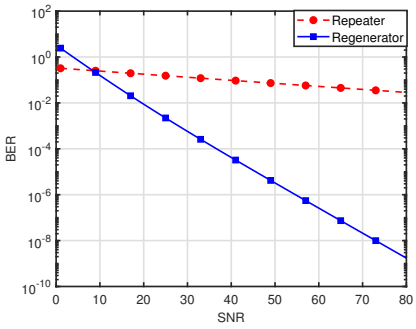

(b) Using Chiani et al's approximation for Q() function in Eq. 8 [Reworked in Eq. 9]

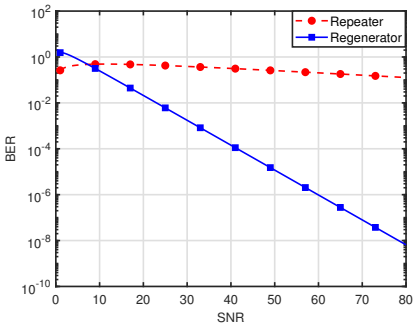

(c) Using Karagiannidis et al's approximation for Q() function in Eq. 8 [Reworked in Eq. 11]

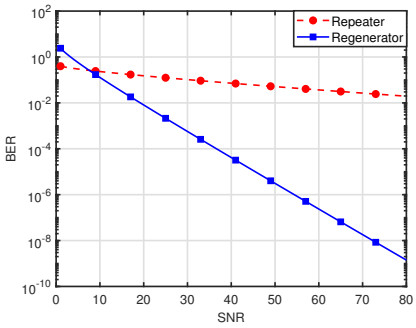

(d) Using Abreu's approximation for Q() function in Eq. 8 [Reworked in Eq. 14]

Fig. 2: BER using Q() function approximations

the section to arrive at numerical results. $\lambda = 1550\,\text{nm}$, $R = 1A/W$, $k_B = 1.38 \times 10^{-23}\,J/K$; $T = 300\,K$, $F_n = 2$, $\Delta f = 5\,GHz$; $R_L = 1\,K\Omega$, $q = 1.602 \times 10^{-19}C$; $P_{in} = 100\,nW$; $G = 10$; $n_{sp} = 1$; $h = 6.626 \times 10^{-34}\,J.s$ and $c = 3 \times 10^8\,m/s$.

Fig. 3 illustrates the important BER vs. input power performance of all-repeater/regenerator link both after a single hop and after M devices. Of course, it is evident that the regenerator link requires much less power to operate at a particular BER as compared to an all-repeater case and more or less retains similar performance with scaling. The repeater link's power requirements increase drastically with the number of hops, as indicated by the red curves being further apart (M = 10 here). The results are in agreement with that of Fig. 1a, and 1c as the all-regenerator link has lower BER for given input power and also degrades much less with scaling.

Next, we compare how BER accumulates over all-repeater and regenerator links using the above-mentioned physical parameters in Eq. 28 and Eq. 21, respectively and corresponding results are shown in Fig. 4a. It is again evident that the regenerator link can operate at much superior BER at all link lengths (at $P_{in} = -25\ dBm$). Additional input power only exacerbates the performance contrast. Additionally, SNR degradation in all repeater links for different input power levels using Eq. 27 is plotted in Fig. 4b. All power levels suffer

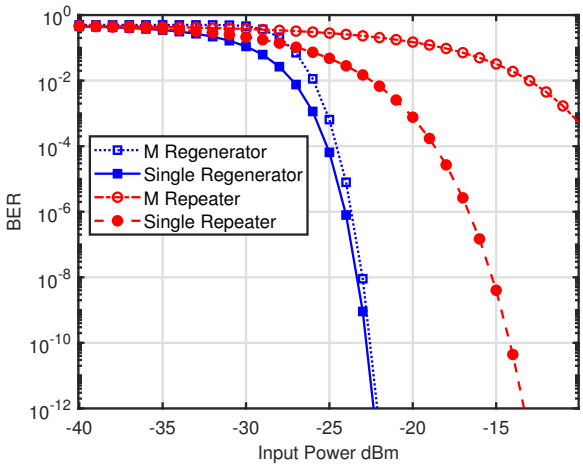

Fig. 3: BER vs Input Power for all Repeater/Regenerator link - After single hop and M = 10

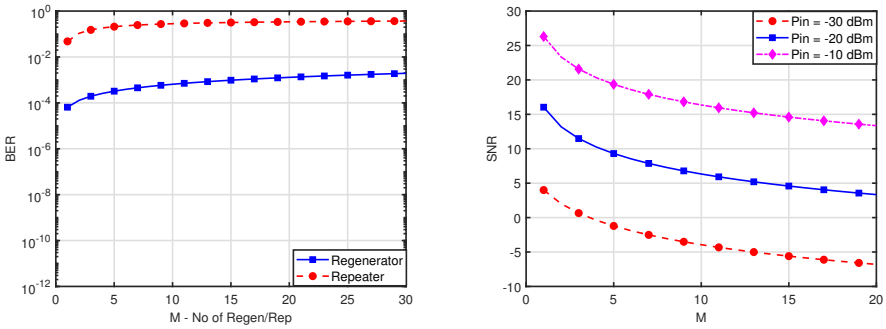

(a) BER accumulation in M (10) Repeater/Regenerator Links

(b) Repeater SNR degradation along the link for different input powers

Fig. 4: BER accumulation and SNR degradation in all Repeater/Regenerator links

similar degradation, which is expected as most of the noise mechanisms discussed are not input signal-dependent (assuming thermal noise limited systems).

The superior BER performance of all-regenerator links can be translated into longer reach or lower power requirements as compared to the all-repeater case as described in section 2.3 and 2.4 respectively. The extra reach corresponding to all-regenerator optical links over the all-repeater optical link for a target BER of 10^{-5} is presented in Fig. 5. There is a sharp peak for regenerator link at around -25 dBm, which is around the minimum power required by a long regenerator link (M >1) as per Fig. 3. As discussed before (about Fig. 3), the regenerator link can support much larger link lengths without an appreciable increase in input power. A staircase shape for repeater scaling can be attributed to reach (M - integer) increment needing a rather drastic improvement in input power for overcoming the noise added in between.

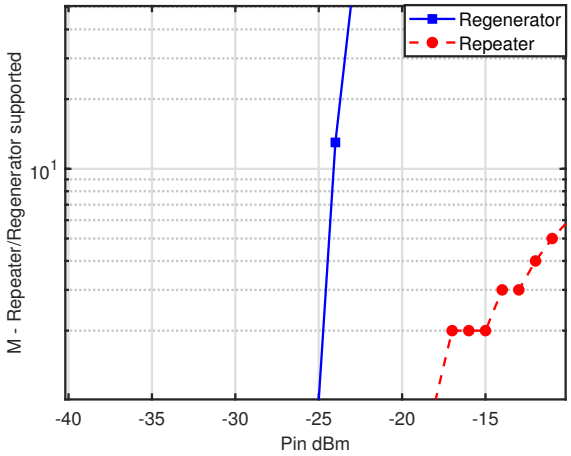

Fig. 5: Link reach vs input power (BER target - 10^{-5}) for all Repeater/Regenerator links

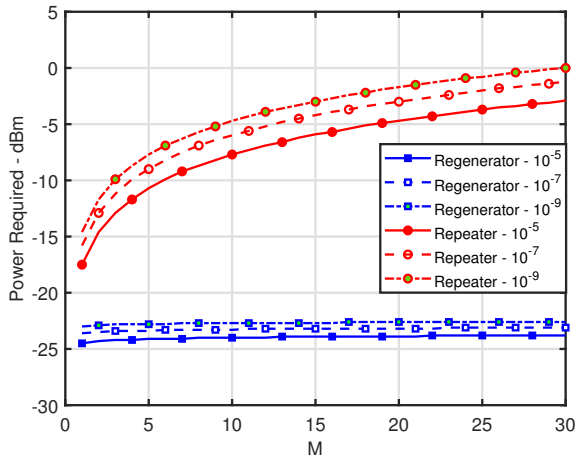

Fig. 6: Power Required for Repeater/Regenerator link for achieving a particular BER

A similar story unveils in Fig. 6 again, where each increment for repeater reach requires quite more power than regenerator link; at all the different BER targets considered. This is because of the high SNR the all-regenerator link can maintain (with only a minor increase in bit errors) throughout the link. Note that, as was evident from the previous results, scaling the all-regenerator link doesn't demand much input power overhead at all.

Varying physical parameters allows us to observe how the link performance changes with different operational conditions. In Fig. 7 we plot the BER at the output of 10 repeater/regenerator link for a thermally limited system, with results from Fig. 3 (M = 10) given for comparison. In this case, the thermal noise dominates the noise terms (of Eq. 27 and Eq. 20) for both repeater and regenerator. Comparing the results shows that shot noise

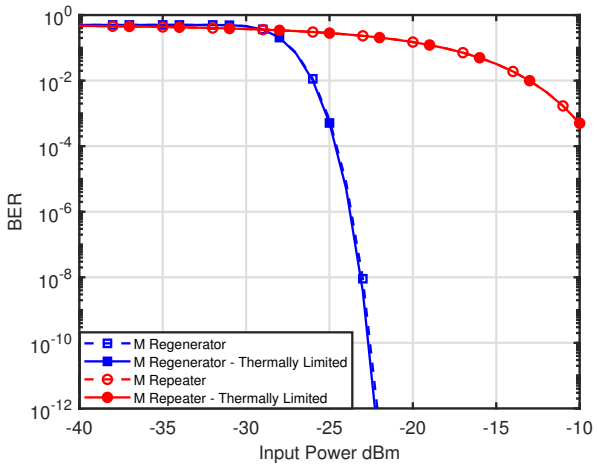

Fig. 7: BER vs Input Power for thermally limited all-repeater/regenerator link

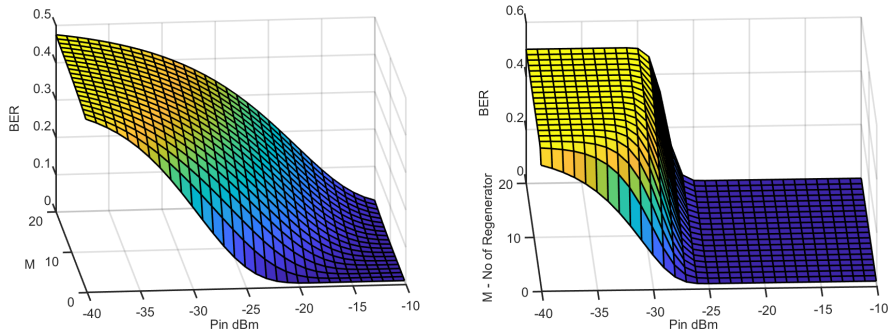

(a) All-Repeater link (b) All-Regenerator link

Fig. 8: Multiparameter plots showing all-Repeater/Regenerator link performance at different input power levels and link lengths

has little bearing in the overall link performance (with everything else kept the same) as both the plots are almost overlapping (normal and thermally limited case) for repeater (red) and regenerator (blue) link. This is particularly the case with all-repeater links where the ASE term in the noise expression dominates (Eq. 20), and hence only one red curve is observable.

A lot of the above results can be consolidated into 3-D plots presented in Figures 8a and 8b, where the BER performance is plotted against input power and link reach simultaneously. The sharper slope of all-regenerator link signifying the drastic scalability of the link for more or less the same input power. These multi-parameter plots give a complete picture for a system designer, which could help make better-informed decisions on different operating parameters. This may also prove to be a versatile tool for predicting performance impacts during link extensions or upgrades.

7 Conclusions

In this paper, we undertake the analytical derivation for the theoretical bounds on BER for both all-regenerator and all-repeater optical links. We prove the superiority of the all-regenerator link and derives the maximum theoretical performance for both cases. Some of the practical limitations of such systems are expected to be overcome in the near future, and we expect the performance to inch closer to the ideal BER at a particular SNR and link reach. Then, we translate this BER advantage of the all-regenerator link into (a) extra reach or (b) lower transmission power. The corresponding results illustrate the design procedure's versatility in specifying the design regarding other performance measures apart from the BER performance. We also introduced approximations for the derived analytical expressions, reducing the computational overhead while estimating the performance measures. Though the computational overhead is not crucial for designing static optical networks (in which the design could be offline), for dynamic optical networks design (wherein the design is real-time), this might prove helpful.

The study involved two different abstractions: the first one a theoretical treatment of the performance bounds; in the latter, we do a proof-of-concept analysis of all-repeater/regenerator links using realistic physical parameters included in the theoretical model. The latter approach also throws light into different noise sources and how they translate into BER down the link. Notably, it was observed in both abstractions that the all-regenerator link could be scaled appreciably with very little increase in input optical power. We have also provided multi-parameter results for quick-glance link performance monitoring and can provide insights into potential performance uplifts with future link upgrades.

Acknowledgements We express our heartfelt thanks to Lakshmi Narayanan Venkatasubramani for all the insights and fruitful discussions.

Declarations

Funding

Not applicable

Availability of data and material

Not applicable

Code availability

Not applicable

Conflict of interest

The authors declare that they have no conflict of interest.

References

1. Abreu G (2012) Very simple tight bounds on the q-function. IEEE transactions on communications 60(9):2415–2420
2. Agrawal GP (2012) Fiber-optic communication systems, vol 222. John Wiley & Sons
3. Agrell E, Secondini M (2018) Information-theoretic tools for optical communications engineers. In: 2018 IEEE Photonics Conference (IPC), IEEE, pp 1–5
4. Botez D, Herskowitz GJ (1980) Components for optical communications systems: A review. Proceedings of the IEEE 68(6):689–731
5. Carlson AB (2010) Communication system. Tata McGraw-Hill Education
6. Chiani M, Dardari D, Simon MK (2003) New exponential bounds and approximations for the computation of error probability in fading channels. IEEE Transactions on Wireless Communications 2(4):840–845
7. Dat PT, Kanno A, Yamamoto N, Kawanishi T (2018) Seamless convergence of fiber and wireless systems for 5g and beyond networks. Journal of Lightwave Technology 37(2):592–605
8. Desai P, Phillips A, Sujecki S (2012) Modeling of burst mode 2r optical regenerator cascades for long-haul optical networks. Journal of Optical Communications and Networking 4(4):304–313
9. Desurvire E, Simpson JR (1989) Amplification of spontaneous emission in erbium-doped single-mode fibers. Journal of lightwave technology 7(5):835–845
10. Desurvire E, Simpson JR, Becker P (1987) High-gain erbium-doped traveling-wave fiber amplifier. Optics letters 12(11):888–890
11. Desurvire E, Giles CR, Simpson JR (1989) Gain saturation effects in high-speed, multichannel erbium-doped fiber amplifiers at lambda= 1.53 mu m. Journal of lightwave technology 7(12):2095–2104
12. Hecht J (2002) Optical regeneration will be key for 40 gbit/s success. Laser focus world 38(4):75–78
13. Jinno M, Takara H, Kozicki B (2009) Dynamic optical mesh networks: drivers, challenges and solutions for the future. In: 2009 35th European Conference on Optical Communication, IEEE, pp 1–4
14. Karagiannidis GK, Lioumpas AS (2007) An improved approximation for the gaussian q-function. IEEE Communications Letters 11(8):644–646
15. Kise T, Nguyen KN, Garcia JM, Poulsen HN, Blumenthal DJ (2011) Cascadability properties of mzi-soa-based all-optical 3r regenerators for rz-dpsk signals. Optics express 19(10):9330–9335
16. Leclerc O (2003) Optical vs. electronic in-line signal processing in optical communication systems: An exciting challenge for optical devices. Signal 1:0
17. Li L, Patki PG, Kwon YB, Stelmakh V, Campbell BD, Annamalai M, Lakoba TI, Vasilyev M (2017) All-optical regenerator of multi-channel signals. Nature Communications 8(1):1–11
18. Liu X, Effenberger F (2016) Emerging optical access network technologies for 5g wireless. Journal of Optical Communications and Networking 8(12):B70–B79
19. Manivasakan R, Francis F (2020) Noise analysis and comparison of an 'm'repeated/regenerator link. In: 2020 IEEE International Conference on Advanced Networks and Telecommunications Systems (ANTS), IEEE, pp 1–6
20. Matsumoto M (2011) Fiber-based all-optical signal regeneration. IEEE Journal of Selected Topics in Quantum Electronics 18(2):738–752

21. Mork J, Ohman F, Bischoff S (2003) Analytical expression for the bit error rate of cascaded all-optical regenerators. IEEE Photonics Technology Letters 15(10):1479–1481
22. Ohlen P, Berglind E (1997) Noise accumulation and ber estimates in concatenated nonlinear optoelectronic repeaters. IEEE Photonics Technology Letters 9(7):1011–1013
23. Parmigiani F, Provost L, Petropoulos P, Richardson DJ, Freude W, Leuthold J, Ellis AD, Tomkos I (2011) Progress in multichannel all-optical regeneration based on fiber technology. IEEE Journal of Selected Topics in Quantum Electronics 18(2):689–700
24. Parmigiani F, Slavík R, Kakande J, Petropoulos P, Richardson D (2015) Optical Regeneration, Springer International Publishing, Cham, pp 129–155
25. Patki P, Guan P, Li L, Lakoba T, Oxenloewe LK, Vasilyev M, Galili M (2020) Recent progress on optical regeneration of wavelength-division-multiplexed data. IEEE Journal of Selected Topics in Quantum Electronics
26. Saleh A, Jopson R, Evankow J, Aspell J (1990) Modeling of gain in erbium-doped fiber amplifiers. IEEE Photonics Technology Letters 2(10):714–717
27. Schiess M, Berglind E, Karlsson A, Thylen L (1996) Pulse shape evolution and noise estimates in concatenated fiber links using analog optoelectronical repeaters. Journal of lightwave technology 14(7):1621–1629
28. Wey JS, Zhang J (2018) Passive optical networks for 5g transport: technology and standards. Journal of Lightwave Technology 37(12):2830–2837
29. Yariv A (1990) Signal-to-noise considerations in fiber links with periodic or distributed optical amplification. Optics letters 15(19):1064–1066
30. Zhu Z, Funabashi M, Pan Z, Xiang B, Paraschis L, Yoo S (2008) Jitter and amplitude noise accumulations in cascaded all-optical regenerators. Journal of lightwave technology 26(12):1640–1652